March 1982

Are VPd_3 and $NbPd_3$ itinerant ferromagnets?

W.L. Burmester
University of Nebraska - Lincoln

David J. Sellmyer
University of Nebraska-Lincoln, dsellmyer@unl.edu

Are VPd_3 and $NbPd_3$ itinerant ferromagnets?[a)]

W. L. Burmester and D. J. Sellmyer

Behlen Laboratory of Physics, University of Nebraska, Lincoln, Nebraska 68588

Low-field magnetic susceptibility and high-field magnetization results are reported for polycrystalline samples of $NbPd_3$, VPd_3, and iron doped VPd_3. Recent self-consistent, spin-polarized band calculations have predicted that the pure compounds are itinerant ferromagnets. Down to 1.6 K there is no evidence for either magnetic ordering or exchange enhancement in VPd_3 and $NbPd_3$. The Fe-doped alloys exhibit transitions at low temperatures to a magnetic cluster-glass state.

PACS numbers: 75.10.Lp, 75.30.Cr, 75.30.Hx

INTRODUCTION

Magnetism in metallic conductors has developed along two paths, the Heisenberg local-moment picture and the Bloch-Slater-Stoner model. In recent years the local-spin-density-function theory has been able to provide impressive advances in understanding the groundstate properties of the elemental ferromagnets, as reviewed recently by Edwards (1) and Pettifor (2). However, at finite temperatures there are still significant controversies concerning the importance of single particle excitations, spin waves, and spin fluctuations. The spin-fluctuation theories of Moriya and coworkers are specifically designed to be able to handle itinerant magnets in the intermediate region between the local-moment and Stoner limits (3).

Band theoretical methods should be most applicable to the class of weak itinerant magnets which are those for which the relative magnetization at absolute zero is much less than unity. A number of materials such as $ZrZn_2$, Sc_3In, Ni_3Al, $TiBe_2$, MnSi, and YNi_3 have been proposed as examples of weak itinerant magnets. These compounds all exhibit some of the characteristic features of the Stoner-Wohlfarth-Edwards theories (2).

The present experimental study was motivated by a recent theoretical development reported by Williams *et al.* (4) These authors describe an alternative to the Stoner model, called "covalent magnetism," which resulted from augmented-spherical-wave calculations done in a self-consistent spin-polarized fashion. The calculations showed that the rigid-band aspect of Stoner theory (similar shapes of up and down density-of-states curves) was not valid. In particular, by examining a series of compounds of the form TPd_3, where T = Ru, Mo, V, Nb, they found that for VPd_3 the density of states at the Fermi level, $n(E_F)$, was large in the paramagnetic state and that the spin-polarized calculations converged to give a moment μ_s of about 1.4 μ_B per formula unit. The Stoner mechanism could account for only a small portion of this total moment. Similar calculations for $NbPd_3$ gave $\mu_s = 0.9\ \mu_B$. (5) Because of the relatively small number of known itinerant magmetic compounds, we have prepared samples of pure VPd_3 and $NbPd_3$ for comparison with the theory. In addition, several samples of Fe-doped VPd_3 were prepared and measured to search for exchange enhancement effects such as those in Pd(Fe) alloys, and to study the nature of the magnetic transitions induced by the iron.

EXPERIMENTAL METHODS

Alloys of $NbPd_3$ and $Fe_xV_{1-x}Pd_3$ were prepared by arc melting in a copper hearth. The materials used were 99.93% Nb powder, 99.7% V flakes, 99.999% Fe rod, and 99.99% Pd sponge. The pure elemental powders were melted into small pellets before weighing to insure that material was not lost in the melting process. The vanadium flakes were heated to near melting temperature under vacuum to remove surface oxidation. The alloys were melted several times in an argon atmosphere. The final weight of the alloy (approx. 2 grams) was within 0.1% of the weight of the starting materials. The phase diagrams show order-disorder transformations at about 1600 °C for $NbPd_3$ (6) and 840 °C for VPd_3 (7). $NbPd_3$, and the $Fe_xV_{1-x}Pd_3$ alloys were annealed for 2-3 weeks at a temperature of 1050 and 700 °C, respectively.

Ordered VPd_3 and $NbPd_3$ have the $TiAl_3$ structure as shown in Fig. 1. The $TiAl_3$ structure has been indexed by two different unit cells, face-centered and body-centered tetragonal. The c_o lengths are the same for the two cells, and a_o lengths are related by a factor of $\sqrt{2}$ (6-8). The annealed samples were polycrystalline with a grain size of about 0.5 mm. The $TiAl_3$ structure was verified on a 114.6 mm Debye-Scherrer camera using a Gondolfi type (9) rotation attachment to produce powder patterns from polycrystalline materials with large grain sizes. Lattice spacings and intensities for VPd_3 have been reported by Dwight *et al.* (8)

Magnetic susceptibility measurements were made with a Faraday-method susceptibility system (10) consisting of a 10 kOe electromagnet with gradient pole

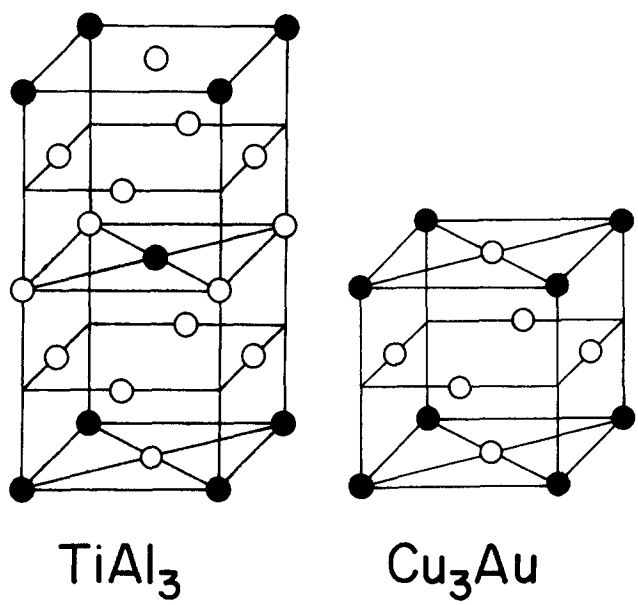

Fig. 1. Unit cells for $TiAl_3$ and Cu_3Au.

 0021-8979/82/032024-03$02.40

pieces, a variable-temperature dewar, and a microbalance. ac susceptibility measurements were made at a field of 0.3 Oe in a balanced coil system of standard design. A lock-in detector was used for excitation and detection at a frequency of 270 Hz. Temperature was varied by lowering the apparatus in a liquid helium storage dewar. High-field magnetization measurements (11) were made with a 80 kOe superconducting magnet in a variable temperature dewar.

EXPERIMENTAL RESULTS AND DISCUSSION

Faraday susceptibility results, $\chi(T)$ at 10.4 kOe, are shown in Fig. 2 for $NbPd_3$. A Curie-Weiss fit to the data gives a temperature-independent susceptibility, χ_0, of 0.69 μemu/g; Curie constant, C, of 1.9 μemu/gK; and a Weiss temperature, θ, of -9.7K. The Curie-Weiss behavior at low temperatures can be accounted for by 65 ppm, or .0065% of magnetic (spin 2) impurities, which is consistent with the purities of the starting materials. At the lowest temperature achieved, 1.6K, no evidence for a magnetic transition was detected.

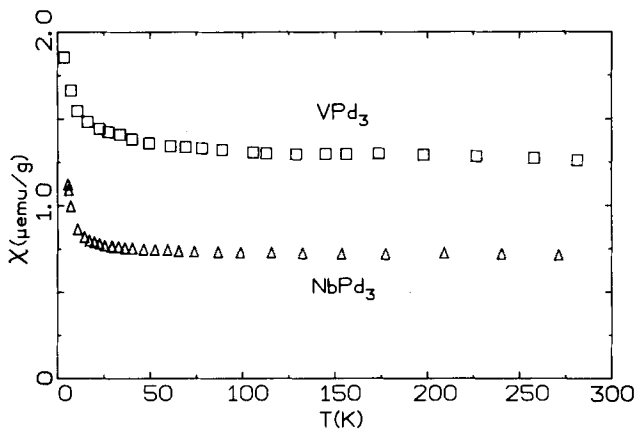

Fig. 2. Faraday susceptibility for VPd_3 and $NbPd_3$.

$\chi(T)$ data at H = 3.2 kOe for VPd_3 are also shown on Fig. 2. The data for VPd_3 are similar to $NbPd_3$, with the former having a larger temperature independent susceptibility and a larger Curie constant. A Curie-Weiss fit to the data gives values for χ_0, C and θ of 1.27 μemu/g, 6.3 μemu/gK, and -7.5K, respectively. The Curie-Weiss behavior can be accounted for by 190 ppm or 0.019% of spin 2 impurities.

VPd_3 was doped with iron to determine if there was an exchange enhancement of the susceptibility. Faraday-method susceptibility measurements at H = 3.2 kOe for $Fe_xV_{1-x}Pd_3$ where x = 0.01, 0.05 are shown in Fig. 3. The x = 0.01 doped sample shows no evidence of order down to 1.6K, and the x = 0.05 doped sample shows a possible spin-glass-type ordering at 2K. Results of Curie-Weiss fits to the data are summarized in Table I. The effective moments are 4.4 μ_B and 4.8 μ_B for the x = 0.01 and x = 0.05 iron doped samples, respectively. These moments are close to the spin-only moment of Fe^{2+}, 4.9 μ_B, implying that there is little or no exchange enhancement in the VPd_3 system.

TABLE I

Curie-Weiss Parameters for $Fe_xV_{1-x}Pd_3$

	χ_0 (μemu/g)	$P_{eff/Fe}$ (μ_B)	θ (K)	T_o* (K)
x=0	1.27	---	-7.5	-
x=.01	1.35	4.4	-2.4	-
x=.05	1.1	4.8	2.1	2
x=.20	-6.3	7.2	29.	6

*T_o = apparent magnetic ordering temperatures

$\chi(T)$ data for $Fe_{0.20}V_{0.80}Pd_3$ are shown in Fig. 4. The sample has a susceptibility maximum at 6K. ac susceptibility data are shown in the insert of Fig. 4. Results of Curie-Weiss fits are listed in Table I, fitted in the temperature range of (50-300K). The x = 0.20 Fe sample does not fit a Curie-Weiss law very well; a low temperature fit (20-50K) gives an effective moment of 38 μ_B/Fe, and a higher temperature region (75-175K) gives an effective moment of 8.2 μ_B/Fe. This can be attributed to different local environments of the Fe atoms, which leads to some large cluster moments as the temperature is lowered.

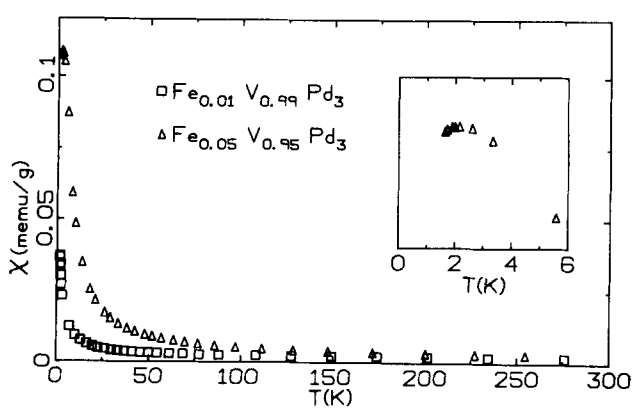

Fig. 3. Faraday susceptibility for $Fe_xV_{1-s}Pd_3$ where x = 0.01, 0.05.

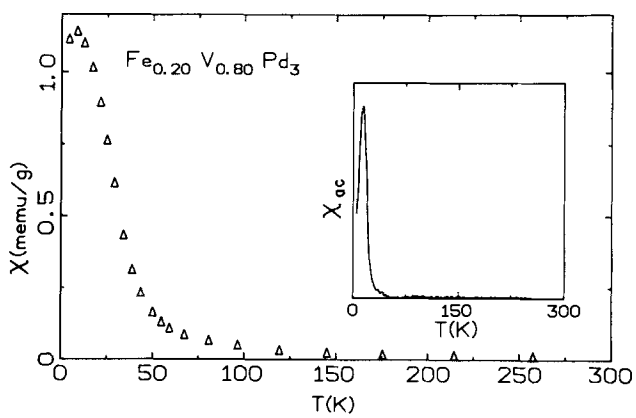

Fig. 4. Faraday and ac susceptibility for $Fe_{0.20}V_{0.80}Pd_3$.

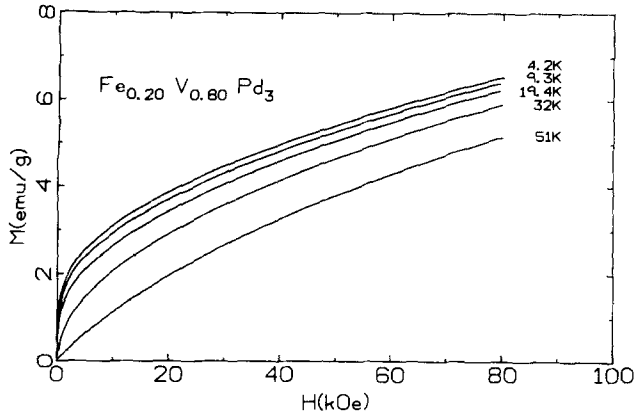

Fig. 5. High field magnetization for $Fe_{0.20}V_{0.80}Pd_3$.

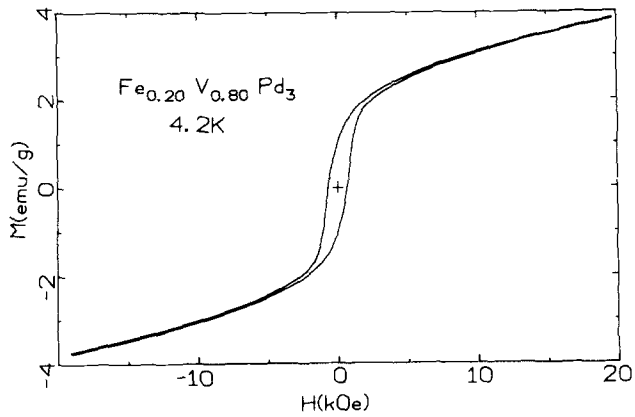

Fig. 6. Hysteresis loop for $Fe_{0.20}V_{0.80}Pd_3$.

High-field magnetization data for $Fe_{0.20}V_{0.80}Pd_3$ as a function of temperature is shown in Fig. 5, and Fig. 6 shows a hysteresis loop at 4.2K. The sharp initial rise in the magnetization at low T and low H, followed by a slow approach to saturation can be attributed to an alignment of the cluster moments at low fields, with an anisotropy, possibly an intercluster exchange anisotropy of the type discussed by Fert and Levy, (12) limiting the saturation of the magnetization at the highest fields. The moment at H = 80 kOe and T = 4.2K is 2.15 μ_B/Fe, with a remanence of 0.35 μ_B/Fe.

The nature of the ordered magnetic state in the $Fe_{0.20}V_{0.80}Pd_3$ alloy appears to be best described as a magnetic cluster glass. The ac susceptibility shows clearly that the susceptibility does not diverge at T_0, which would lead to a flat "measured" susceptibility below T_0 = 6K. Yet the apparent spin-glass-like transition is not consistent with a standard spin glass of the Cu(Mn) or Au(Fe) type. This is evident from the ferromagnetic-like high-field magnetization curves seen in Figs. 5 and 6, in which about 2 μ_B per Fe atom is developed at high fields. The magnetic cluster glass appears to be a state in which there are strong ferromagnetic intracluster interactions and weak intercluster interactions which can be overpowered by a field of order 10^4 Oe. Although no microscopic measurements have been performed, the suggested model most likely would involve an inhomogeneous magnetic state in which atomic short range order between Fe atoms is significant.

CONCLUSIONS

We have found no evidence for magnetic ordering in VPd_3 or $NbPd_3$. Iron doping of VPd_3 shows no evidence of exchange enhancement. The band calculations of Williams et al. were performed assuming the 4 atom/cell Cu_3Au structure (Fig. 1) whereas VPd_3 and $NbPd_3$ have the 8 atom/cell $TiAl_3$ structure. The difference in the V or Nb local environments could account for the theoretical predictions and the experimental results. A calculation of the band structure using the $TiAl_3$ structure would be useful, to see what effect the structure has on the results, and to see if the discrepancy with experimental results can be resolved.

Finally, the magnetic state of the $Fe_xV_{1-x}Pd_3$ alloys appears to be, in the dilute case, one of ordinary Fe^{2+} localized moments on Fe atoms, and in the increasingly concentrated case, one of a magnetic cluster glass with significant atomic short range order.

ACKNOWLEDGMENTS

We are grateful to S.G. Cornelison and Z.D. Chen for help with the measurements and to the National Science Foundation for financial support.

REFERENCES

a) Research supported by NSF Grants DMR-7810781 and DMR-8110520.
1) D.M. Edwards, J. Magn. and Magn. Mat. 15-18, 262 (1980).
2) D.G. Pettifor, J. Magn. and Magn. Mat. 15-18, 847 (1980).
3) T. Moriya, J. Magn. and Magn. Mat. 14, 1 (1979).
4) A.R. Williams, R. Zeller, V.L. Moruzzi, and C.D. Gelatt, Jr., J. Appl. Phys. 52, 2067 (1981).
5) R. Zeller, private communication.
6) B.C. Giessen, N.J. Grant, D.P. Parker, R.D. Manuszewski, and R.M. Waterstrat, Met. Trans. A, 11A, 709 (1980).
7) R.P. Elliott, Constitution of Binary Alloys, First Supplement (McGraw-Hill, New York, 1965).
8) A.E. Dwight, J.W. Downey, and R.A. Conner, Jr., Acta Cryst. 14, 75 (1961).
9) G. Gandolfi, Miner. Petrogr. Acta, 13, 67 (1967).
10) F.R. Szofran, W.L. Burmester, D.J. Sellmyer, and L.G. Rubin, Rev. Sci. Instrum. 46, 1186 (1975).
11) J.A. Gerber, W.L. Burmester, and D.J. Sellmyer, to be published.
12) A. Fert and P.M. Levy, Phys. Rev. Lett. 44, 1538 (1980).